THE JOURNAL OF BIOLOGICAL CHEMISTRY VOL. 287, NO. 24, pp. 20056–20069, June 8, 2012

Estradiol Protects Dermal Hyaluronan/Versican Matrix during Photoaging by Release of Epidermal Growth Factor from Keratinocytes*[S]

Received for publication, February 14, 2012, and in revised form, March 23, 2012 Published, JBC Papers in Press, April 9, 2012, DOI 10.1074/jbc.M112.353151

Katharina Röck[‡], Michael Meusch[‡], Nikola Fuchs[‡], Julia Tigges[§], Petra Zipper[¶], Ellen Fritsche[§], Jean Krutmann[§], Bernhard Homey[¶], Julia Reifenberger[¶], and Jens W. Fischer[‡1]

From the [‡]Institut für Pharmakologie and Klinische Pharmakologie, Universitätsklinikum Düsseldorf, Heinrich-Heine-Universität Düsseldorf, the [§]IUF-Leibniz Institute for Environmental Medicine, and the [¶]Department of Dermatology, Universitätsklinikum Düsseldorf, Heinrich-Heine-Universität Düsseldorf, 40225 Düsseldorf, Germany

Background: Skin aging involves UVB-induced degeneration of the dermal extracellular matrix.
Results: Estrogen induces epidermal growth factor expression in keratinocytes thereby stimulating hyaluronan synthase 3 and versican expression in dermal fibroblasts of UVB-irradiated skin.
Conclusion: Paracrine release of epidermal growth factor in response to estrogen maintains hyaluronan and versican-rich extracellular matrix.
Significance: Estrogen prevents specific aging responses in the hyaluronan matrix of photoaged skin.

Hyaluronan (HA) and versican are key components of the dermis and are responsive to ultraviolet (UV)B-induced remodeling. The aim of this study was to explore the molecular mechanisms mediating the effects of estrogen (E_2) on HA-rich extracellular matrix during photoaging. Hairless skh-1 mice were irradiated with UVB (three times, 1 minimal erythema dose (80 mJ/cm^2), weekly) for 10 weeks, and endogenous sex hormone production was abrogated by ovariectomy. Subcutaneous substitution of E_2 by means of controlled-release pellets caused a strong increase in the dermal HA content in both irradiated and nonirradiated skin. The increase in dermal HA correlated with induction of HA synthase HAS3 by E_2. Expression of splice variant 2 of the HA-binding proteoglycan versican was also increased by E_2. In search of candidate mediators of these effects, it was found that E_2 strongly induced the expression of epidermal growth factor (EGF) in UVB-irradiated epidermis *in vivo* and in keratinocytes *in vitro*. EGF in turn up-regulated the expression of HAS3 and versican V2 in dermal fibroblasts. HAS3 knockdown by shRNA caused inhibition of fibroblast proliferation. Furthermore, HAS3 and versican V2 induction by E_2 correlated positively with proliferation *in vivo*. In addition, the accumulation of inflammatory macrophages, expression of inducible cyclooxygenase 2, as well as proinflammatory monocyte chemotactic protein 1 were decreased in response to E_2 in the dermis. Collectively, these data suggest that E_2 treatment increases the amount of dermal HA and versican V2 via paracrine release of EGF, which may be implicated in the pro-proliferative and anti-inflammatory effects of E_2 during photoaging.

Photoaging of the skin inevitably occurs at sun-exposed areas such as the face, neck, and hands. This process is characterized by intrinsic and extrinsic aging responses and by an overlap with photo-carcinogenesis under certain circumstances (1). The role of the ECM[2] of the skin in this aging process is well established. In particular, the cleavage of collagen by matrix metalloproteinases has been demonstrated (2). The partially degraded collagen network heals imperfectly through *de novo* collagen synthesis, leaving microscars in the skin. Collagen fragments that are released as a result of matrix metalloproteinase-induced collagen cleavage are bioactive and participate in the regulation of fibroblast phenotype during photoaging. Moreover, collagen fragments reduce *de novo* synthesis of dermal collagen (3). Thus, matrix degradation and altered matrix expression influence fibroblast phenotypes and may thereby perpetuate UVB-induced aging responses. Other dermal ECM molecules are also reportedly affected by UVB irradiation, particularly hyaluronan (HA) and proteoglycans (4–7). HA is abundant in the dermis and is thought to contribute to water content, turgidity of the skin, and the diffusion of soluble factors and nutrients (5). Furthermore, HA can support the proliferative phenotype of fibroblasts and possibly opposes apoptosis (8, 9). HA is synthesized at the plasma membrane by HA synthase isoenzymes-1, -2, and -3 (HAS1–3) (10). These enzymes extrude HA into the extracellular space after assembly of UDP-glucuronic acid and UDP-*N*-acetyl-D-glucosamine into a growing chain of β(1–3)-linked D-glucuronic acid and *N*-acetyl-D-glucosamine disaccharides. The repeating disaccharides are linked by hexosaminidic β(1–4) bonds that form high molecular weight HA of up to 10^7 Da and up to 20 μm in length (11). HAS isoenzymes are expressed at a relatively low copy number per cell but can rapidly produce large amounts of HA. In addition to transcriptional regulation of HAS enzymes, it has recently been shown that regulation also takes place at the

* This work was supported by Deutsche Forschungsgemeinschaft Grants SFB 728, TP C6, C1, and C4.
[S] This article contains supplemental Figs. 1 and 2.
[1] To whom correspondence should be addressed. Tel.: 49-211-8112500; Fax: 49-211-8114781; E-mail: jens.fischer@uni-duesseldorf.de.

[2] The abbreviations used are: ECM, extracellular matrix; OVX, ovariectomy; HAS, hyaluronan synthase; E2R, E_2 receptor; S, sham; P, placebo; X, OVX; bHABP, bovine HA-binding protein; RHAMM, receptor of HA-mediated motility; DAB, 3,3′-diaminobenzidine; HA, hyaluronan.

post-transcriptional level through phosphorylation, glycosylation, and mono-ubiquitination (12–14). Furthermore the formation of homo- and heterodimers has now been demonstrated (13).

With respect to skin aging, it has been shown that HA is reduced by chronic UVB irradiation, and this loss likely contributes to the aged phenotype of skin (8, 15–17). However, a limited number of studies have also demonstrated either no change or increased dermal HA in response to UVB (15, 18). The latter is likely an acute response associated with heliodermatitis.

Hyaluronan is bound by versican, a large chondroitin sulfate proteoglycan, through specific binding domains termed link modules that each consist of ~100 amino acids and are part of the link protein domain. The link protein domain is composed of an immunoglobulin domain and two link modules and is present in the N-terminal globular G1 domain of versican (19). Because multiple versican molecules bind to one chain of HA, large networks of HA and versican are formed. These HA and versican-rich matrices are known to critically govern the proliferative and migratory phenotype of mesenchymal cells (20). Recently, it has been demonstrated that versican accumulates in response to UVB irradiation (7). However, little is known about what the specific functions of versican might be during skin aging, how versican is regulated during skin aging, and specifically whether versican is responsive to estrogen.

Skin aging is accelerated after menopause and positive effects on the skin including increased thickness, increased moisture, decreased wrinkling, and improved wound healing responses became obvious upon estrogen treatment of postmenopausal women (21). However, hormone replacement therapy is confounded by thrombotic and malignant complications and is now restricted to short term use in selected cases (22). It is therefore of great interest to better understand the molecular mechanisms that underlie the protection of the skin matrix by E_2. The aim of this study was to investigate the effect of E_2 on the dermal hyaluronan and versican matrix during UVB-induced skin aging by use of ovariectomized and E_2 treated hairless skh-1 mice.

EXPERIMENTAL PROCEDURES

UVB Irradiation of Mice—Female hairless mice (Skh:Hr1) (Charles River Laboratories) were housed according to standard procedures. Mice were randomly assigned to either sham procedure or bilateral ovariectomy (OVX, X) at the age of 8 weeks as described previously (23). OVX mice were subdivided into four treatment groups, which received either placebo or E_2 ± UVB irradiation. E_2 treatment was performed by implantation of subcutaneous slow release hormone pellets (Innovative Research of America) prepared to dispense 1.1 μg/day E_2 for the duration of the 10-week experimental period. Placebo (P) pellets served as control. After OVX and pellet implantation at 8 weeks, half of the mice were irradiated with UVB light and the other half served as nonirradiated controls. Sham-operated animals received placebo pellets ± UVB irradiation. Thus, six experimental groups (Fig. 1*A*) were compared in total as follows: 1) sham, placebo (*S,P*); 2) OVX, placebo (*X,P*); 3) OVX, E_2 (*X,*E_2); 4) sham, placebo, UVB (*S,P UVB*); 5) OVX, placebo, UVB (*X,P UVB*); and 6) OVX, E_2, UVB (*X,*E_2 *UVB*).

Animals were exposed to UVB radiation in an irradiation chamber as described previously (8) using UV lamps with fluorescent bulbs (280–320 nm with a peak at 313 nm TL 20W/12; Philips, Eindhoven, The Netherlands). UVB irradiation was performed three times per week at a dose of 80 mJ/cm^2 (irradiation time 1 min 36 s) equaling one minimal erythema dose over a period of 10 weeks (Fig. 1*A*). The light intensity was determined by means of a UV meter (Waldmann, Villingen-Schwennigen, Germany). Skin biopsies from the dorsal skin of 1 × 1.5 cm^2 in size were obtained from control and UVB-irradiated animals after 10 weeks. All animal experiments were approved by the local ethical committee for animal experiments.

Histology—Skin biopsies were frozen in tissue freezing medium (Leica Nussloch, Bensheim, Germany) in liquid isopentane at −40 °C, and 12-μm cryosections were prepared for immunohistochemical staining. Affinity histochemistry of HA was performed with bovine HA-binding protein (bHABP, Seikagaku, Tokyo, Japan) and detected with biotin-labeled streptavidin (2 μg/ml, Calbiochem). The following primary antibodies were used: Versican (LF99, 1:400, rabbit anti-human, kindly provided by Dr. Larry Fisher, NIDCR, National Institutes of Health, Bethesda); HAS3 (H64, 1:500, Santa Cruz Biotechnology, Santa Cruz, CA); MAC-2 (1:250, Cedarlane, Burlington, Canada); KI-67 (1:50, Novus Biological, Littleton, CO), and COX2 (1:1000, Cayman, Ann Arbor, MI). The respective biotinylated secondary antibodies (1:1000) were obtained from Calbiochem. Detection was performed using 3,3′ diaminobenzidine (Zytomed, Berlin, Germany) as a chromogen. Nuclei were stained with hemalaun solution (Merck). Negative controls without the primary antibody were performed for every antigen. No staining was detectable in the papillary dermis of any of these control stainings (data not shown).

Digital image analysis was performed using a modified approach based on Dai *et al.* (8). Bright field images (8-bit) of the stained sections were captured using a Leica DM2000 microscope (Leica Microsystems, Wetzlar, Germany) at ×100 magnification. For the quantification of the staining intensity, ImageJ software 1.41 Version (National Institutes of Health) was used according to instructions of ImageJ. The color deconvolution plug-in was employed to separate the color channels of hemalaun and DAB. Negative controls and strongly DAB-positive images were used to determine the thresholds and the analyzed range of signals. This procedure minimized the background interference and maximized the signal of DAB-positive tissue. Thresholds were set for the complete analysis of one antigen. The area fraction is defined as percentage of the area classified as DAB-positive. The measurement was performed in the papillary dermis excluding regions that contained hair follicles. Per skin section data from three randomly selected areas were averaged.

Cell Culture—Human dermal fibroblasts from female donors were purchased from PromoCell (Heidelberg, Germany), maintained in monolayer cultures in Dulbecco's modified Eagle's medium (DMEM) without phenol red (Sigma), and supplemented with 10% heat-inactivated, charcoal-treated fetal

bovine serum, 2 mmol/liter L-glutamine, and antibiotics (100 units/ml penicillin, 50 mg/ml streptomycin-G). Normal human epidermal keratinocytes were purchased from PromoCell and cultured in keratinocyte media 2 (PromoCell). The cells were maintained at 37 °C, 5% CO_2 and 95% humidified air.

UVB irradiation of the cells was performed with a Bio-Sun irradiation system (Vilbert Lourmat, Munich, Germany) containing two 30-watt UVB sources (312 nm). During the UVB irradiation procedure (100 mJ/cm^2; irradiation time ~10 s), cells were kept in phosphate-buffered saline solution, which was replaced by DMEM containing 10% charcoal-treated FCS with or without 100 nM β-estradiol (Sigma) immediately after the irradiation. Cells were harvested 24 h after stimulation.

For the cell media transfer experiments, NEHKs were UVB-irradiated and stimulated with E_2 as described above in keratinocyte media 2. The supernatant was collected 24 h after stimulation and was transferred to fibroblasts in the presence or absence of erlotinib (3 μM) (LC Laboratories, Woburn, MA), EGF-neutralizing antibody, or IgG isotype control (both 0.35 μg/ml, Abcam, Cambridge, UK). Fibroblasts were harvested 24 h after exposure to conditioned media.

RNA Isolation and Quantification of Gene Expression—Total RNA was isolated using RNeasy total RNA kits (Qiagen, Hilden, Germany). The RNA concentration was determined via photometric measurement at absorbance 260/280. Total RNA (1 μg) was reverse-transcribed using the SuperscriptIII first-strand synthesis system for reverse transcriptase-PCR (RT-PCR) (Invitrogen). Primers to analyze target mRNA expression levels were designed employing Primer Express 3.0 software (Applied Biosystems, Darmstadt, Germany) based on published mRNA sequences. The sequences are given in Table 1. Real time RT-PCR was performed in triplicate using SYBR Green PCR master mix (Applied Biosystems) as described (15). The $2^{-\Delta\Delta C(T)}$ method was used for comparison of the relative expression between control and treated cells. A melting curve analysis was performed after every run, and a negative control containing only master mix, the primer pair, and water was included on every plate.

Knockdown of HAS3—*HAS3* knockdown was achieved by usage of the MISSION^{TM} lentiviral shRNA knockdown system (Sigma) as described previously (24). A scrambled shRNA served as control, and the anti-*HAS3* hairpin sequence was 5′-CGGGCTCTACAACTCTCTGTGGTTCTCGAGAACCACAGAGAGTTGTAGAGCTTTTTG-3′.FuGENE 6 (Roche Applied Science) was used for the transfer into the packaging cell line HEK293T (ATCC, Wesel, Germany). For better stability of the produced lentiviral particles, the medium was changed to Iscove's modified Dulbecco's medium after 16 h. The lentiviruses were harvested 24 h later and concentrated by centrifugation with poly-L-lysine as reported previously (25). Fibroblasts were transfected with a multiplicity of infection of 5 and kept in normal growth medium for at least 5 days before stimulation with conditioned keratinocyte medium. Before using the cells in proliferation assays, the efficacy of the lentiviral *HAS3* knockdown was verified by quantitative RT-PCR (data not shown) and Western blot analysis (anti-HAS3, 1:1000, Sigma) (supplemental Fig. 1).

TABLE 1
Primer sequences used for quantification of gene expression
f indicates forward, and r indicates reverse.

Gene	Primer sequence
Human *CD44*	f, 5′-GCTATTGAAAGCCTTGCAGAG-3′ r, 5′-CGCAGATCGATTTGAATATAACC-3′
Human *COX2*	f, 5′-TGAGTGTGGGATTTGACCG-3′ r, 5′-TGTGTTTGGAGTGGGTTTCA-3′
Human *EGF*	f, 5′-AGTTTTTCTGAATGGGTCAAGG-3′ r, 5′-TCCAATTTATTGCCATTCCAG-3′
Human *GAPDH*	f, 5′-GTGAAGGTCGGAGTCAACG-3′ r, 5′-TGAGGTCAATGAAGGGGTC-3′
Human *HAS1*	f, 5′-TACAACCAGAAGTTCCTGGG-3′ r, 5′-CTGGAGGTGTACTTGGTAGC-3′
Human *HAS2*	f, 5′-GTGGATTATGTACAGGTTTGTGA-3′ r, 5′-TCCAACCATGGGATCTTCTT-3′
Human *HAS3v1*	f, 5′-GAGATGTCCAGATCCTCAACAA-3′ r, 5′-CCCACTAATACACTGCACAC-3′
Human *HYAL1*	f, 5′-CCAAGGAATCATGTCAGGCCATCAA-3′ r, 5′-CCCACTGGTCACGTTCAGG-3′
Human *HYAL2*	f, 5′-GGCTTAGTGAGATGGACCTC-3′ r, 5′-CCGTGTCAGGTAATCTTTGAG-3′
Human *RHAMM*	f, 5′-GAATATGAGAGCTCTAAGCCTG-3′ r, 5′-CCATCATACTCCTCATCTTTGTC-3′
Human pan-*VERSICAN*	f, 5′-AGACTGTCAGATATCCCATCC-3′ r, 5′-AATCCATAAGTCCTGACTCCT-3′
Human *VERSICAN V1*	f, 5′-CGTCGAATGAGTGATTTGAG-3′ r, 5′-TTTCAGCCATTAGATCATGCAC-3′
Human *VERSICAN V2*	f, 5′-AAGACAGGACCTGATCGCT-3′ r, 5′-AGTGGCTCCATTACGACAGG-3′
Human *VERSICAN V3*	f, 5′-ACGACCTGATCGCTGCAA-3′ r, 5′-CAAGTGGCTCCATTACGACA-3′
Human *VERSICAN Vo*	f, 5′-ACCAGGACCTGATCGCTGCAA-3′ r, 5′-GTTCATTTTGCAGCGATCAG-3′
Murine *Cd44*	f, 5′-CAAGTTTTGGTGGCACACAG-3′ r, 5′-CTGTAGCGGCCATTTTTCTC-3′
Murine *Cox2*	f, 5′-CCGGACTGGATTCTATGGTG-3′ r, 5′-CCTTGAAGTGGGTCAGGATG-3′
Murine *Egf*	f, 5′-GCCACGCTTACATTCATTCC-3′ r, 5′-ATCGCCTTGCTTTTCAACAC-3′
Murine *E2Rα*	f, 5′-AGCTGCTCCTCCACTTGGT-3′ r, 5′-GGCGTCGATTGTCAGAATTAG-3′
Murine *E2Rβ*	f, 5′-TACGGTGTCTGGTCCTGTGA-3′ r, 5′-TACACTGATTCGTGGCTGGA-3′
Murine *Gapdh*	f, 5′-TGGCAAAGTGGAGATTGTTGCC-3′ r, 5′-AAGATGGTGATGGGCTTCCCG-3′
Murine *Has1*	f, 5′-TATGCTACCAAGTATACCTCG-3′ r, 5′-TCTCGGAAGTAAGATTTGGAC-3′
Murine *Has2*	f, 5′-CGGTCGTCTCAAATTCATCTG-3′ r, 5′-ACAATGCATCTTGTTCAGCTC-3′
Murine *Has3*	f, 5′-GATGTCCAAATCCTCAACAAG-3′ r, 5′-CCCACTAATACATTGCACAC-3′
Murine *Hyal1*	f, 5′-AAGTACCAAGGAATCATGCC-3′ r, 5′-CTCAGGATAACTTGGATGGC-3′
Murine *Hyal2*	f, 5′-GGTGGACCTTATCTCTACCAT-3′ r, 5′-TATTGGCAGGTCTCCATACTT-3′
Murine *Il6*	f, 5′-GATGGATGCTACCAAACTGGA-3′ r, 5′-GGTACTCCAGAAGACCAGAGGA-3′
Murine *Ki-67*	f, 5′-CCAGCTGTCCTCAAGACAATC-3′ r, 5′-CACTGGAAGTCCTGCCTGAT-3′
Murine *Mac-2*	f, 5′-TGAGAGTGGCAAACCATTCA-3′ r, 5′-GTCACCACTGATCCCCAGTT-3′
Murine *Mcp-1* (*CcL2*)	f, 5′-CCCAATGAGTAGGCTGGAGA-3′ r, 5′-TCTGGACCCATTCCTTCTTG-3′
Murine *Rhamm*	f, 5′-GCCACTCAGAAGGACCTCAC-3′ r, 5′-TGCACAGCTAATTTCTTGGATG-3′
Murine *Tgfβ1*	f, 5′-CTAATGGTGGACCGCAACA-3′ r, 5′-ACTGCTTCCCGAATGTCTGA-3′
Murine *Tgfβ2*	f, 5′-CGAGGAGTACTACGCCAAGG-3′ r, 5′-GTAGAAAGTGGGCGGGATG-3′
Murine *Tgfβ3*	f, 5′-TTCGACATGATCCAGGGACT-3′ r, 5′-TCTCCACTGAGGACACATTGA-3′
Murine *Tnfα*	f, 5′-CGAGTGACAAGCCTGTAGCC-3′ r, 5′-AGCTGCTCCTCCACTTGGT-3′
Murine *Tpx2*	f, 5′-TCCCTGGATGCTAAGAGAGC-3′ r, 5′-TTTCAACAGAGGCAACATGG-3′
Murine pan-*Versican*	f, 5′-ACCATGTCACTGGCTGTGG-3′ r, 5′-AGCGGCAAAGTTCAGAGTGT-3′
Murine *Versican V1*	f, 5′-GCCTACTGCTTTAAACGTCGA-3′ r, 5′-GCAAACAGATCATGCAGTGG-3′
Murine *Versican V2*	f, 5′-ACAGGACCTGATCTCTGCAAAA-3′ r, 5′-CCATTCCGACAAGGGTTAGA-3′
Murine *Versican V3*	f, 5′-ACGACCTGATCTCTGCAA-3′ r, 5′-CCATTCCGACAAGGGTTAGA-3′
Murine *Versican Vo*	f, 5′-AAGACAGGTCGATTGAGTGATAT-3′ r, 5′-GCAAACAGATCATGCAGTGG-3′

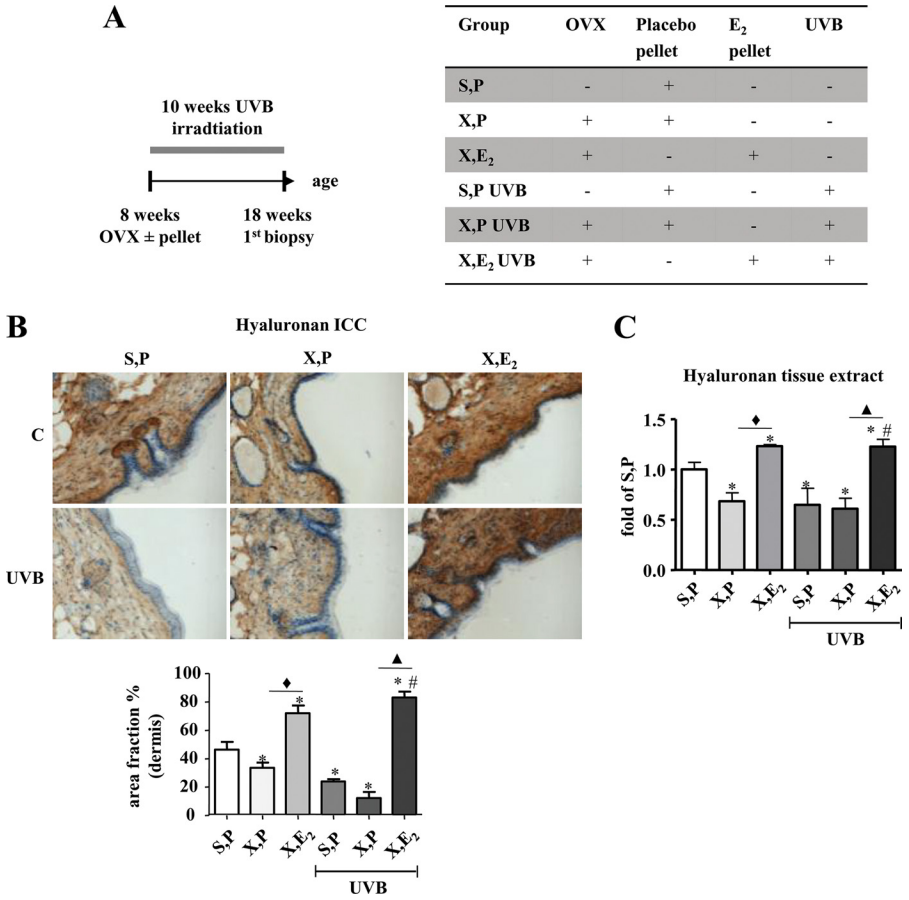

Group	OVX	Placebo pellet	E_2 pellet	UVB
S,P	-	+	-	-
X,P	+	+	-	-
X,E_2	+	-	+	-
S,P UVB	-	+	-	+
X,P UVB	+	+	-	+
X,E_2 UVB	+	-	+	+

FIGURE 1. **Induction of HA by E_2 *in vivo*.** Hairless skh-1 mice were ovariectomized (OVX, X) at the age of 7–8 weeks or were sham-operated (*S*). Ovariectomized and sham-operated animals received either a subcutaneous placebo pellet (*P*) as control or a subcutaneous long release E_2 pellet (1.1 μg E_2/day/mouse) (E_2). Subsequently, mice were subjected to UVB irradiation (three times 1 minimal erythema dose, weekly) for 10 weeks. At age of 18 weeks, skin biopsies were obtained, and the amount of HA was quantified. *A,* experimental protocol and abbreviations. *B,* affinity histochemistry of the skin using biotinylated bHABP and quantitative analysis (area fraction) of HA staining in the papillary dermis. *C,* measurement of HA in skin extracts using a bHABP-based kit. ×100 magnification; $n = 7–12$, mean ± S.E.; *, $p < 0.05$ *versus* S,P; #, $p < 0.05$ *versus* S,P UVB; ♦, $p < 0.05$ *versus* X,P; ▲, $p < 0.05$ *versus* X,P UVB.

Determination of HA and EGF in Cell Culture Supernatants—HA concentration in the supernatants was determined using an HA test kit based on bHABP (Corgenix, Peterborough, UK) 24 h after stimulation and was normalized to total cellular protein. The EGF concentration in the supernatants was determined by EGF human ELISA kit (Abcam, Cambridge, UK) according to the manufacturer's protocol 24 h after stimulation.

Immunoblotting—In equal aliquots of cell culture supernatants or skin extracts, versican was first enriched by DEAE ion exchange chromatography and was chondroitin ABC lyase-digested, and subsequently core proteins were separated on SDS-PAGE and Western blotted as described previously (26). LF99 (1:1000) was used as primary antibody.

HAS3 was detected by immunoblotting using anti-HAS3 antibody (H64, 1:1000 Santa Cruz Biotechnology) for murine samples and anti-HAS3 antibody (1:1000 Sigma) for human samples. β-Tubulin antibody was from Sigma (1:1000, Munich). MAC-2 was from Cedarlane (1:250, Burlington, Canada), and COX2 was from Cayman (1:1000, Ann Arbor, MI). Primary antibodies were detected by infrared fluorescent-coupled secondary antibodies (1:5000 LI-COR, Bad Homburg, Germany) allowing fluorescent detection using the LI-COR Odyssey Infrared Imaging System.

Determination of HA and EGF in Murine Skin—For HA extraction from murine skin, biopsies were lyophilized; the dry weight was determined, and samples were digested by Pronase (protease from *Streptomyces griseus*, 6 mg/ml in 100 mmol/liter Tris-HCl, pH 8, 1 mmol/liter $CaCl_2$, and 1500 units/ml heparin, 60 °C, 24 h; Sigma). HA was subsequently ethanol-precipitated (12 h, −20 °C) and recovered by centrifugation (10,000 × *g*, 4 °C, 15 min). Samples were diluted 1:20,000, and the HA concentration was determined by HA test kit based on bHABP (Corgenix, Peterborough, UK) and normalized to dry weight (27).

For determination of EGF, murine skin lysates were prepared by homogenization in modified RIPA buffer (50 mM Tris-HCl, pH 7.4, 1% Triton X-100, 0.2% sodium deoxycholate, 0.2% SDS, 1 mM sodium EDTA, 1 mM phenylmethylsulfonyl fluoride, 5 μg/ml aprotinin, 5 μg/ml leupeptin). Tissue and cell debris was removed by centrifugation. EGF concentrations were determined by EGF mouse ELISA kit (Abcam, Cambridge, UK) according to the manufacturer's protocol. Protein concentrations were determined using the Bio-Rad protein assay (Bio-Rad).

Statistical Analysis—All data sets were analyzed by one-way analysis of variance and the Bonferroni post hoc test. Data pre-

sented in Fig. 5 were analyzed by Student's *t* test. Data are presented as means ± S.E., and statistical significance was assigned at the level of $p < 0.05$.

RESULTS

E_2 Elevates Dermal HA in UVB-irradiated and Nonirradiated Skin—Hairless skh-1 mice were ovariectomized to deplete endogenous sex hormones. The lack of E_2 was substituted in OVX mice by implantation of subcutaneous long release pellets (1.1 μg E_2/day/mouse). This nonirradiated group allowed the characterization of the effect of E_2 on the intrinsically aged dermal HA matrix at 18 weeks of age. OVX led to slightly reduced amounts of HA as shown by affinity histochemistry and biochemical quantification in skin extracts (Fig. 1, *B* and *C*). Of note, E_2 substitution substantially elevated dermal HA above the control level (S,P) suggesting a stimulatory effect of E_2.

To investigate the role of estrogen during photoaging, skh1 mice were irradiated with UVB (three times 1 minimal erythema dose (80 mJ/cm2), weekly) for 10 weeks. Subsequently, skin biopsies were collected from UVB-exposed areas. UVB-induced loss of dermal HA (S,P UVB) and again substitution of E_2 prevented the decline of HA (X,E_2 UVB) in a way that HA levels were even higher than those observed in nonirradiated, non-OVX controls (*S,P,* Fig. 1, *B* and *C*).

Dermal HAS3 Expression Is Responsive to E_2 in the Skin of UVB-irradiated and Nonirradiated Mice—To analyze the mechanisms that mediate the elevation of HA content in response to E_2, mRNA expression of *Has* isoenzymes and hyaluronidases (*Hyal*) 1 and 2 were analyzed. Of note, *Has3* mRNA expression was strongly induced by E_2 in nonirradiated and irradiated OVX mice (Fig. 2*A*). HAS1 was significantly down-regulated in OVX mice that received UVB irradiation (X, P UVB). This effect was reversed by E_2, which could therefore contribute to the recovery of HA matrix in E_2-supplemented mice after irradiation (supplemental Fig. 2*A*). *Has2* by contrast was up-regulated after OVX (X, P), which could potentially counteract the loss of HA to some extent. The other conditions examined did not affect *Has2* expression (supplemental Fig. 2*B*). Therefore *Has3* was considered as the most important HAS isoenzyme mediating the recovery of HA matrix after E_2 substitution. Increased *Has3* expression in response to E_2 was also validated at the protein level by immunocytochemistry and immunoblotting. As a result, HAS3 protein detection confirmed the regulation of *Has3* mRNA (Fig. 2, *B* and *C*) by E_2. Western blot analysis detected an additional band below the predicted size of HAS3 (63 kDa). The identity of the band is not known, but the detected protein showed the same expression pattern as the mature HAS3.

Nonirradiated skin also showed induction of *Hyal2* in response to OVX (supplemental Fig. 2*D*), which was prevented by E_2 substitution and could therefore contribute to decreased HA content in response to OVX and the increase of HA in response to E_2 treatment. *Hyal1* was not regulated in a fashion that could explain the observed changes in dermal HA (supplemental Fig. 2*C*). Finally, expression of the HA receptors CD44 and receptor of HA-mediated motility (*Rhamm*) were determined by real time RT-PCR (supplemental Fig. 2, *E* and *F*). *Cd44* expression was found to be unresponsive to both OVX/E_2 and to UVB irradiation. *Rhamm*, however, was down-regulated by UVB irradiation in OVX animals, and E_2 substitution partially restored expression, suggesting that HA signaling via RHAMM is responsive to E_2.

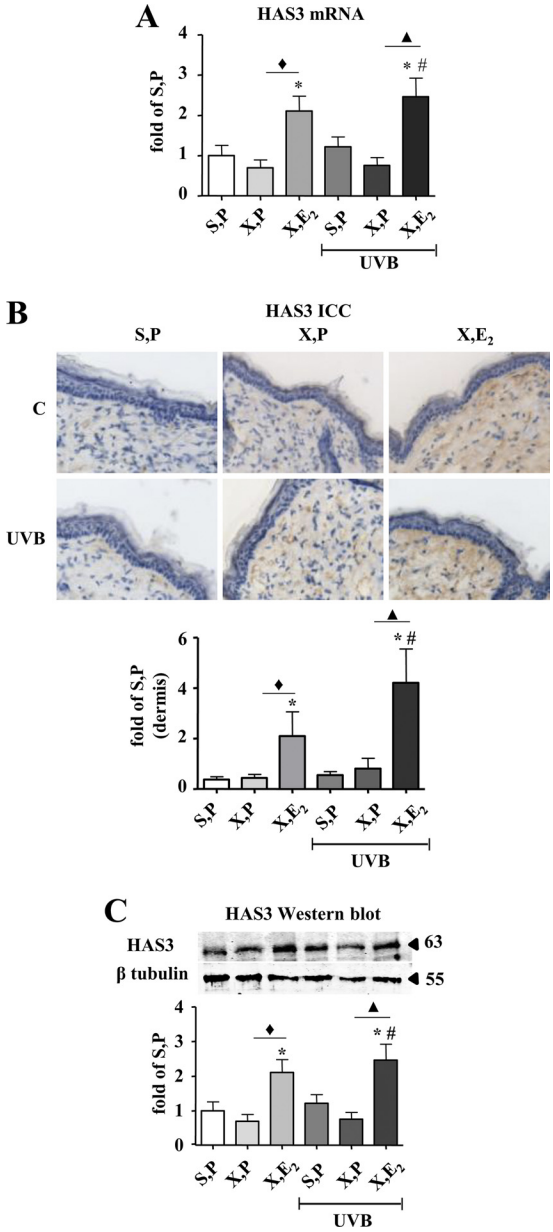

FIGURE 2. **Induction of HAS3 by E_2 *in vivo*.** HAS3 expression was determined in skin biopsies of hairless skh-1 mice that were treated as detailed in Fig. 1. At the age of 18 weeks, skin biopsies were obtained, and the amount of HAS3 was analyzed. *A*, *Has3* mRNA expression in skin extracts. *B,* HAS3 immunostaining and quantitative image analysis of the papillary dermis The 63-kDa band was quantified by densitometry and related to tubulin loading control (55 kDa). *C,* HAS3 immunoblotting (H64) of total skin extracts and quantitative analysis. ×100 magnification; $n = 7–12$, mean ± S.E.; *, $p < 0.05$ *versus* S,P; #, $p < 0.05$ *versus* S,P UVB; ♦, $p < 0.05$ *versus* X,P; ▲, $p < 0.05$ *versus* X,P UVB.

Quantitation of E_2 receptors by real time RT-PCR revealed that E2Rβ was not detectable in the dermis of female hairless skh-1 mice in any of the experimental groups (data not shown). In contrast, the E2Rα receptor (supplemental Fig. 2*G*) was highly abundant, but expression was not affected by any of the experimental interventions. These data suggest that the effects of E_2 were mediated by the E2Rα receptor.

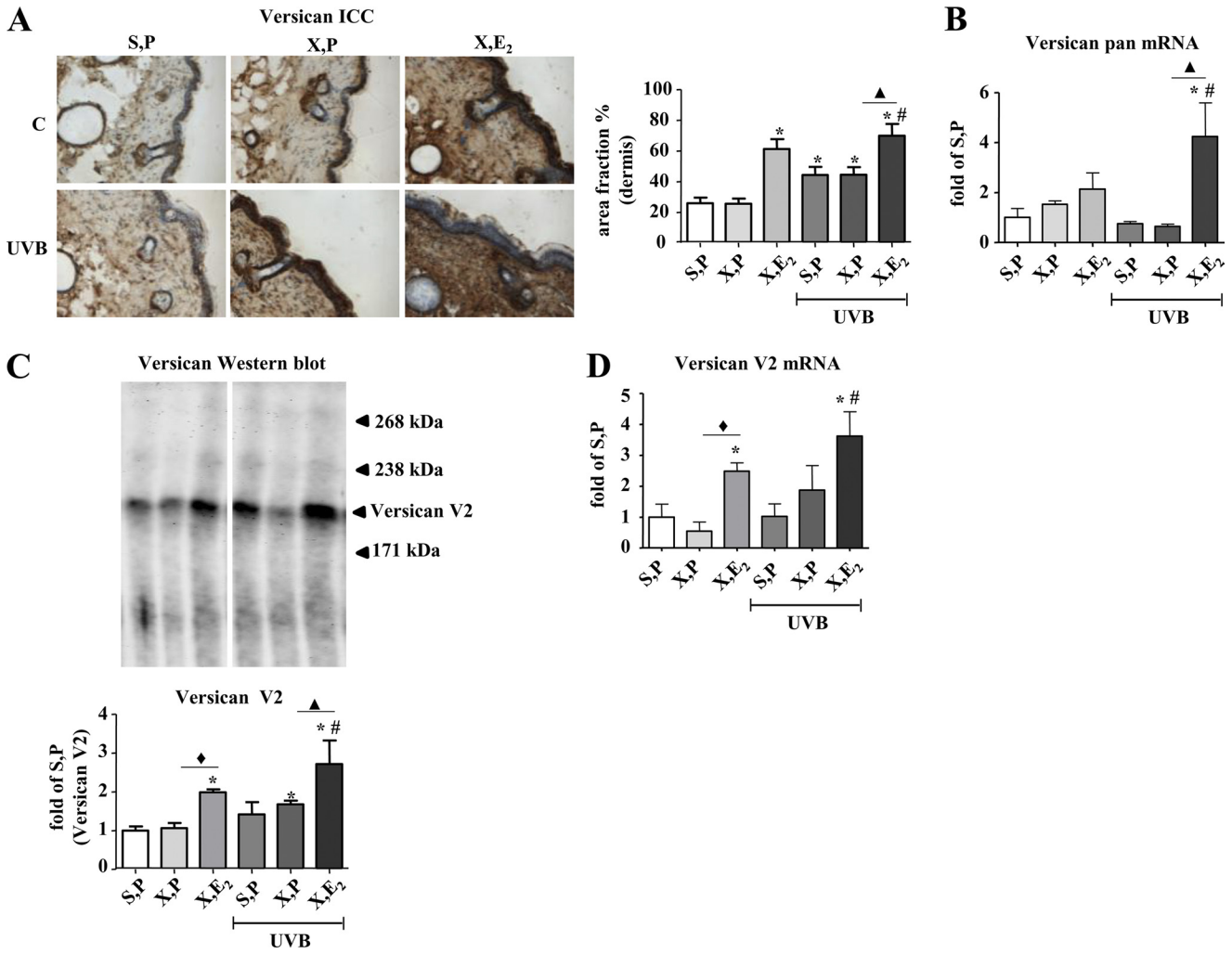

FIGURE 3. **Up-regulation of versican in response to E_2 *in vivo*.** Versican expression was determined in skin biopsies from hairless skh-1 mice that were treated as detailed in Fig. 1. At age of 18 weeks, skin biopsies were obtained, and the amount of versican was analyzed. *A,* pan-versican immunostaining and quantitative image analysis. *B,* mRNA expression of pan-*Versican* in skin extracts. *C,* pan-versican immunoblotting (LF99) from skin extracts (equal aliquots) and quantitative analysis of the main band (V2) between 238 and 171 kDa. *D, Versican V2* mRNA expression in skin extracts. ×100 magnification; $n = 7–12$, mean ± S.E.; *, $p < 0.05$ *versus* S,P; #, $p < 0.05$ *versus* S,P UVB; ♦, $p < 0.05$ *versus* X,P; ▲, $p < 0.05$ *versus* X,P UVB.

E_2 Up-regulates Versican Content in Dermal Matrix—Subsequently, the regulation of the HA-binding proteoglycan versican was characterized. Immunostaining of versican revealed that OVX did not affect versican but that substitution of E_2 caused marked dermal versican accumulation in nonirradiated skin (*X,E_2*, Fig. 3*A*). Furthermore UVB irradiation itself raised the versican content of the dermis in the immunohistochemical staining (Fig. 3*A*), and this was further increased by E_2. Four splice variants of versican (V_0, V_1, V_2, and V_3) are known. To obtain a read-out of the overall versican mRNA expression, a primer that did not distinguish between the splicing variants was initially used. The mRNA expression of pan-*Versican* was not changed or even decreased in response to UVB (Fig. 3*B*), but a trend toward up-regulation was seen in X,E_2 samples, which reached statistical significance in UVB irradiated X,E_2 mice. Immunoblotting of versican in skin extracts revealed a major versican band at ~200 kDa, which likely represented the versican splice variant V2 (Fig. 3*C*) and closely resembled the regulation of versican as evidenced by immunostaining. Therefore, mRNA expression of *Versican* V2 was analyzed by real time RT-PCR (Fig. 3*D*) and found to parallel the protein data shown in Fig. 3, *A* and *C*.

Comparable changes in versican expression were also determined in the epidermis by quantitation of immunostainings (data not shown) suggesting a similar response to E_2 in the epidermis. Therefore, part of the data from whole skin extracts (mRNA and immunoblotting) also reflect increased epidermal versican. In contrast, regulation of HAS3 was not detected in the epidermal compartment (data not shown). Future studies may address the effect of E_2 and versican specifically in the epidermis.

Thus, dermal HA and versican were markedly increased by E_2 in both nonirradiated and irradiated skin. Furthermore, the data suggest that HAS3 and versican V2 are the molecular targets of this regulation. With respect to quantitative remodeling, the UVB-irradiated dermal matrix of OVX mice is characterized by a proportional loss of HA and an increase in versican.

Effects of E_2 on HAS Isoenzymes and Versican in Dermal Fibroblasts in Vitro—The above described *in vivo* results suggest a strong effect of exogenous E_2 on the dermal HA and

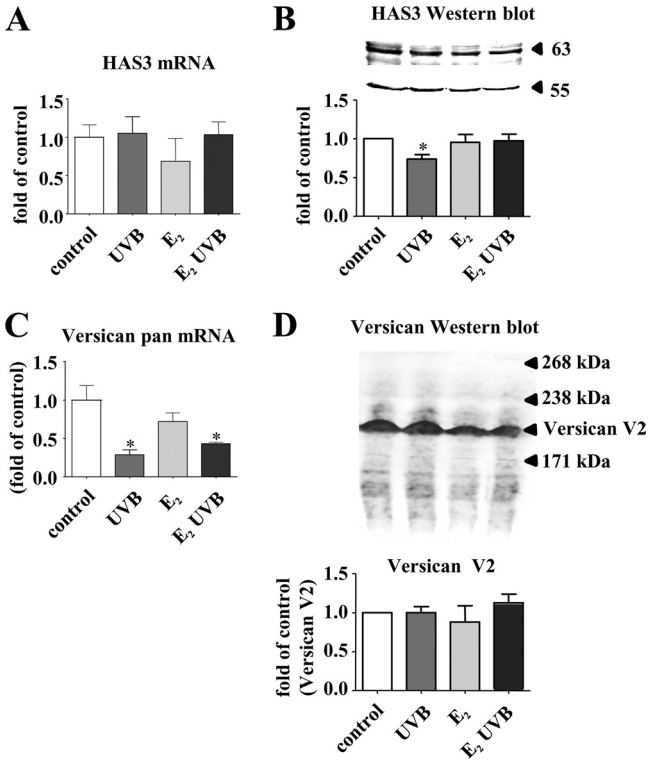

FIGURE 4. **HAS3 and versican expression in human skin fibroblasts in response to UVB and E_2.** Fibroblasts were either untreated, received a single dose of 100 mJ/cm^2 UVB, or 100 nM E_2, or both and were analyzed after 24 h. *A, HAS3* mRNA; *B,* HAS3 immunoblotting (Sigma) and quantitative analysis in relation to tubulin as loading control (55 kDa); *C,* pan-*VERSICAN* mRNA expression; *D,* pan-versican immunoblotting (LF99, equal aliquots) and quantitative analysis of versican V2; $n = 3–6$, mean ± S.E.; *, $p < 0.05$ *versus* control.

versican matrix. In search of the underlying regulatory mechanisms, two possibilities were considered. First, direct transcriptional effects of E_2 on *HAS* isoenzymes and *VERSICAN* in fibroblasts may be responsible. Second, indirect effects of E_2 on the expression of growth factors that may in turn affect gene expression could be involved. Therefore, it was tested whether the *HAS* isoenzymes and *VERSICAN* are responsive to E_2 and UVB *in vitro*. In monolayer cultures of human skin fibroblasts, *HAS3* mRNA was not affected by either UVB or E_2 (Fig. 4*A*), although HAS3 immunoblotting even suggested a slight decrease of HAS3 protein after UVB exposure (Fig. 4*B*). pan-*VERSICAN* mRNA was down-regulated in response to UVB and UVB + E_2 (Fig. 4*C*). However, immunoblotting of versican from supernatants revealed no effect on versican V2 expression (Fig. 4*D*). Therefore, in contrast to the *in vivo* results, HAS3 and versican were clearly not directly induced by E_2 in fibroblasts *in vitro*. Next, concentration-dependent responses of fibroblasts exposed to E_2 and UVB were examined by real time RT-PCR. Using 0.1, 1, 10, and 100 μM E_2 revealed that *HAS3* mRNA was not regulated, whereas *HAS1* and *HAS2* mRNA were even down-regulated in fibroblasts 24 h after stimulation (data not shown). Application of 10, 50, and 100 mJ UVB/cm^2 led to down-regulation of *HAS1* and *HAS2* at 100 mJ/cm^2 and a weak reduction of *HAS3* mRNA at 10 mJ/cm^2 (data not shown). The transcriptional down-regulation of all three *HAS* isoenzymes in response to direct UVB irradiation of fibroblasts could potentially be related to the loss of HA in response to UVB *in vivo*. However, *in vivo* only *Has1* mRNA was slightly reduced in UVB-irradiated skin of X,P mice (supplemental Fig. 2, *A* and *B*). With respect to pan-*VERSICAN* mRNA expression, dose responses revealed that only 100 nM E_2 inhibited expression as seen in Fig. 4*C*, whereas lower concentrations had no effect (data not shown). After UVB irradiation, a small increase of pan-*VERSICAN* mRNA expression (1.39 ± 0.15-fold, $p < 0.05$ compared with control, $n = 3$) was detected at 10 mJ/cm^2, followed by significant inhibition by 100 mJ/cm^2 as presented in Fig. 4*C*. All considered, in cultured fibroblasts neither the estrogen response nor the acute UVB response mimicked the results obtained *in vivo*. Therefore, a direct regulation of the involved genes in fibroblasts by E_2 and UVB appeared unlikely to be responsible for the induction of HA and versican *in vivo* in response to E_2.

EGF Is Induced in Keratinocytes in Response to E_2 and Induces HAS3 and Versican Expression in Fibroblasts—Next, a possible paracrine mechanism was addressed. For this purpose, skin biopsies were examined with regard to differential regulation of growth factors known to be involved in the regulation of the HA matrix. Specifically, it was searched for candidates that were diminished by OVX and increased by E_2 substitution both in nonirradiated and irradiated skin. *Egf* was identified as one candidate that showed reduced mRNA expression in OVX mice, which could be rescued by E_2 in both nonirradiated and UVB-irradiated mice (Fig. 5*D*). EGF protein expression was therefore quantified in skin extracts by ELISA (Fig. 5*E*) confirming the induction by E_2 in nonirradiated and irradiated OVX animals. Furthermore, expression of EGF protein specifically in the epidermis was determined by immunostaining (Fig. 5*F*). The results confirmed that EGF is indeed induced in the epidermis and in total skin extracts by E_2. In contrast, *Tgfβ1–3* mRNA patterns did not correlate with the changes of HA, HAS3, and versican V2 in response to E_2. Therefore, EGF was considered as the most promising candidate for a paracrine mediator released in response to E_2 from keratinocytes that may in turn regulate HAS3 and versican V2 in dermal fibroblasts.

The effect of EGF on dermal fibroblasts was subsequently examined *in vitro*. Fig. 6 shows that EGF induces *HAS3* mRNA, HAS3 protein, and HA synthesis in skin fibroblasts (Fig. 6, *A–C*). On the immunoblots, the same lower molecular weight band as described in Fig. 2*C* was detected. Quantification (data not shown) revealed the same regulation of this smaller protein as the mature HAS3. Furthermore, EGF induced total *VERSICAN* mRNA (Fig. 6*D*), versican V2 protein (Fig. 6*E*), and *VERSICAN V2* mRNA (Fig. 6*F*). Next, it was addressed whether UVB and E_2 affect the release of EGF from keratinocytes. Of note, E_2 induced expression and release of EGF in both nonirradiated and irradiated keratinocytes (Fig. 7, *A* and *B*) as determined by quantitative real time RT-PCR and ELISA. In dermal fibroblasts EGF expression was not stimulated by E_2 and UVB under the current experimental conditions (data not shown). Next, conditioned medium derived from keratinocytes exposed to E_2 and E_2 plus UVB was used to stimulate dermal fibroblasts as illustrated in Fig. 7*C*. The conditioned medium from keratinocytes exposed to E_2 and E_2 plus UVB was found to induce *HAS3* and *VERSICAN V2* mRNA expression (Fig. 7, *D* and *E*).

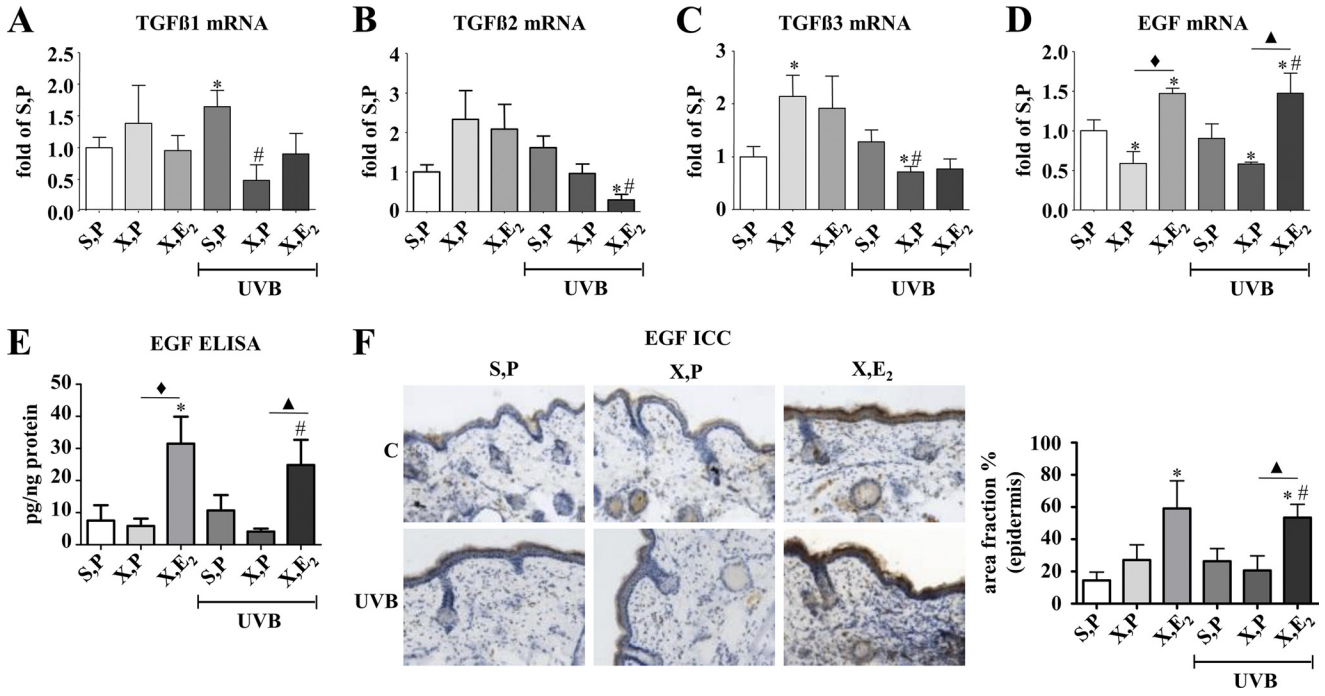

FIGURE 5. **Gene expression profile in skin biopsies in response to UVB and E_2.** Mice were treated as detailed under "Experimental Procedures" and in the legend of Fig. 1. Skin biopsies were obtained at 18 weeks of age, and mRNA expression was determined by real time RT-PCR. *A, Tgfβ1*; *B, Tgfβ2*; *C, Tgfβ3*; *D, Egf*; *E*, EGF protein in skin extracts determined by ELISA; *F*, EGF immunostaining and quantitative image analysis specifically of the epidermis. ×100 magnification; $n = 5–12$, mean ± S.E.; *, $p < 0.05$ *versus* S,P; #, $p < 0.05$ *versus* S,P UVB; ♦, $p < 0.05$ *versus* X,P; ▲, $p < 0.05$ *versus* X,P UVB.

The induction of HAS3 mRNA and versican V2 mRNA was blocked by both an EGF receptor kinase inhibitor, erlotinib, and by a neutralizing antibody against EGF (Fig. 7, *D* and *E*). Furthermore, the supernatants of E_2-treated keratinocytes stimulated the proliferation of fibroblasts as determined by [^{3}H]thymidine incorporation (Fig. 7*F*). This pro-proliferative effect of conditioned medium from E_2-stimulated keratinocytes was EGF-dependent because erlotinib and a neutralizing antibody against EGF were able to block the effect (Fig. 7*F*). Next, it was tested whether HAS3 induction might be responsible for this pro-proliferative effect. Indeed, lentiviral knockdown of *HAS3* (suppression of *HAS3* mRNA to 0.6 ± 0.1-fold of scrambled control, $p < 0.05$, $n = 6$) prohibited proliferative response in fibroblasts induced by the conditioned keratinocyte medium (Fig. 7*G*). Therefore, it is proposed (i) that E_2 induces expression and release of EGF from keratinocytes *in vivo* and (ii) that EGF induces in a paracrine manner HAS3, HA, and versican expression in fibroblasts of the papillary dermis.

Differential Effects of E_2 on Dermal Cell Proliferation and Inflammation—Next, it was attempted to link the specific changes of dermal HA and versican to functional effects in the dermis during photoaging. The proliferation of dermal fibroblasts as determined by Ki-67 immunostaining and mRNA expression was increased by E_2 both in nonirradiated and in UVB-irradiated skin (Fig. 8, *A* and *B*). This was further supported by the induction of *Tpx2* (microtubule-associated homolog) mRNA expression, which is also indicative for proliferative activity (Fig. 8*C*). HA and versican are both thought to contribute to proliferation of dermal fibroblasts (see Fig. 7*G*). It is conceivable that this proliferative response to E_2 is in part due to HA synthesis via HAS3 and possibly also increased versican V2.

It has been suggested that HA plays a role in inflammation either as a result of generation of HA fragments or the formation of supramolecular complexes of HA and HA-binding proteins that form HA cables and allow monocyte/macrophage adhesion. Interestingly, in the UVB-irradiated dermis of OVX mice, which contained a reduced amount of HA and an elevated amount of versican, Mac-2 immunostaining, immunoblotting, and mRNA expression, indicative for macrophage content, were increased (Fig. 9, *A–C*). Furthermore, *Mac-2* mRNA and protein expression were strongly reduced by E_2 suggesting an anti-inflammatory effect of E_2 during skin aging (Fig. 9, *A–C*). To further support this hypothesis, the expression profiles of the chemokines and cytokines *Mcp-1*, *IL6*, and *Tnfα* were analyzed and found to be suppressed in at least one of the E_2-treated groups (Fig. 9, *D--F*). Finally, the expression of inducible cyclooxygenase 2 (*Cox2*) was analyzed as an indicator of inflammatory activity. *Cox2* mRNA expression and protein expression (data not shown) were also strongly suppressed by E_2 (Fig. 9*G*). In summary, the *in vivo* data are consistent with a pro-proliferative and anti-inflammatory effect of estrogen that coincided with induction of both HAS3, HA, and versican in UVB-irradiated skin (Fig. 10).

DISCUSSION

Estrogen has been known for a long time to have beneficial effects on the skin, which is particularly obvious after the onset of menopause or the initiation of estrogen treatment of postmenopausal women (21). Estrogens partially protect from skin aging by increasing thickness, reducing the wrinkling, and augmenting the moisture of the skin (28–30). It has been demonstrated that estrogen treatment prevents loss of collagen type 1 and increases *de novo* collagen synthesis (31). Furthermore,

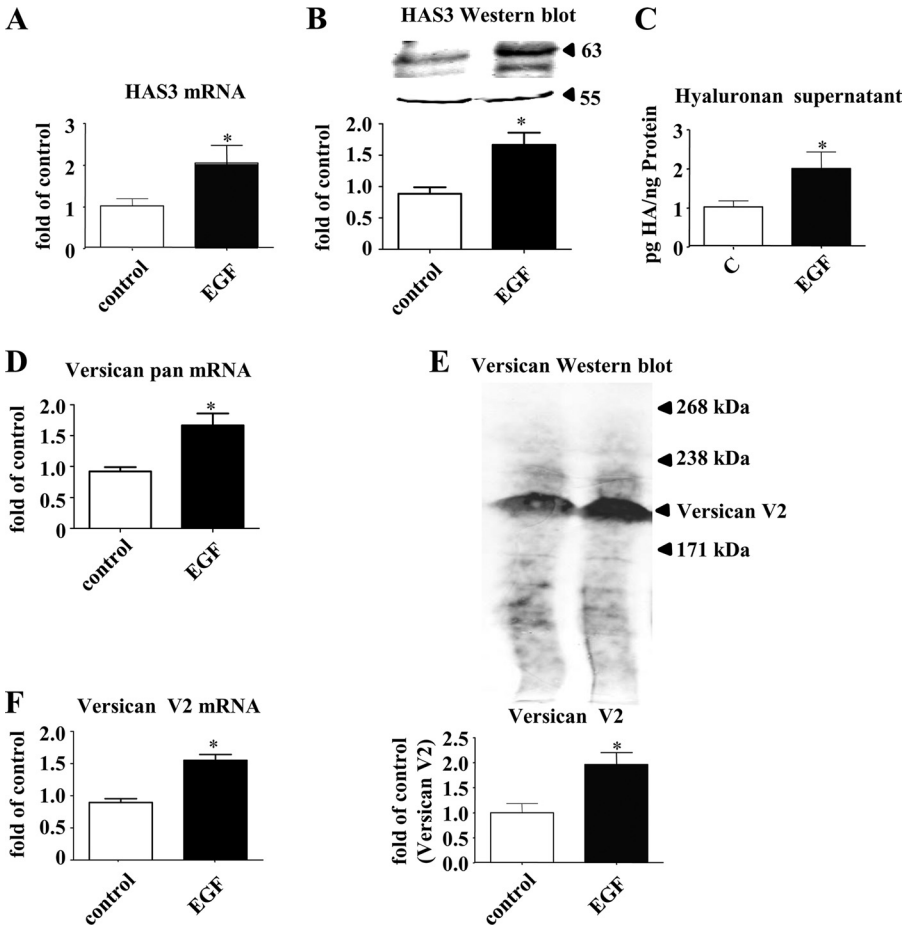

FIGURE 6. **HAS3 and versican expression in human fibroblasts in response to EGF.** Human skin fibroblasts were stimulated with EGF (10 ng/ml) for 24 h. *A, Has3* mRNA expression; *B,* HAS3 immunoblotting (Sigma) and quantitative analysis; *C,* HA secreted into the medium during 24 h after stimulation with EGF; *D,* pan-*VERSICAN* mRNA expression; *E,* pan-versican immunoblotting (LF 99, equal aliquots) and quantitative analysis; *F, VERSICAN* V2 mRNA expression. $n = 3–6$, mean ± S.E.; *, $p < 0.05$ *versus* control.

estrogens increase dermal glycosaminoglycans, which in turn may contribute to the thickness and moisture of the skin (32–34). Loss of HA from the skin appears to be part of the postmenopausal aging response. In male mice, the administration of estrogen increases HA content of the skin (35). However, systematic animal studies in females addressing the regulatory effect of estrogens on dermal HA, HAS isoenzymes, HA receptors, and hyaluronidases and importantly the underlying molecular mechanisms are lacking. Furthermore, to date nothing is known about how E_2 may regulate the content and function of HA and versican in the skin. Therefore, the aim of this study was to investigate changes of HA, HAS isoenzymes, hyaluronidases, HA receptors, and the HA-binding proteoglycan versican in the context of photoaging and E_2.

This study clearly shows that E_2 is a strong inductor of dermal HA and versican in both nonirradiated skin and UVB-irradiated skin in hairless skh-1 mice. Moreover, HAS3 was identified as the responsible target and therefore an important E_2-dependent regulator of dermal HA homeostasis during intrinsic and extrinsic skin aging.

E_2 mediates changes in gene expression by activation of intracellular E2Rα and -β, which translocate into the nucleus upon ligand binding and affect the expression of genes with estrogen response elements in the promoter region. In addition, nongenomic E_2 effects occur through the GPR30 pathway (36). It has been shown that both E2Rα and -β are expressed in the skin and specifically in skin fibroblasts (21). However, considerable variability appears with respect to the ratio of both ER subtypes in various organs, ages, and species (37, 38). Therefore, the expression of *E2R*α and -β was determined by real time PCR in hairless skh-1 mice. The *E2R*α receptor was strongly expressed in the skin biopsies, whereas the *E2R*β receptor was not detectable. Therefore, the above mentioned effects of E_2 on dermal HA and versican during photoaging were attributed to *E2R*α. However, the contribution of nongenomic effects cannot be excluded.

Because the *in vivo* experiments suggested that induction of HAS3 and versican V2 expression likely played a key role in the estrogen response during photoaging, it was addressed whether E_2 directly induced these genes in fibroblasts. However, no evidence for direct transcriptional induction of *HAS3* and *VERSICAN V2* gene expression by E_2 was found. As an alternative explanation, the induction of paracrine factors by E_2 that subsequently induce expression of *HAS3* and *VERSICAN* appeared plausible. This hypothesis is in line with the report that E_2 indeed affects dermal ECM via paracrine mechanisms *in vivo*. It has been shown that postmenopausal loss of collagen

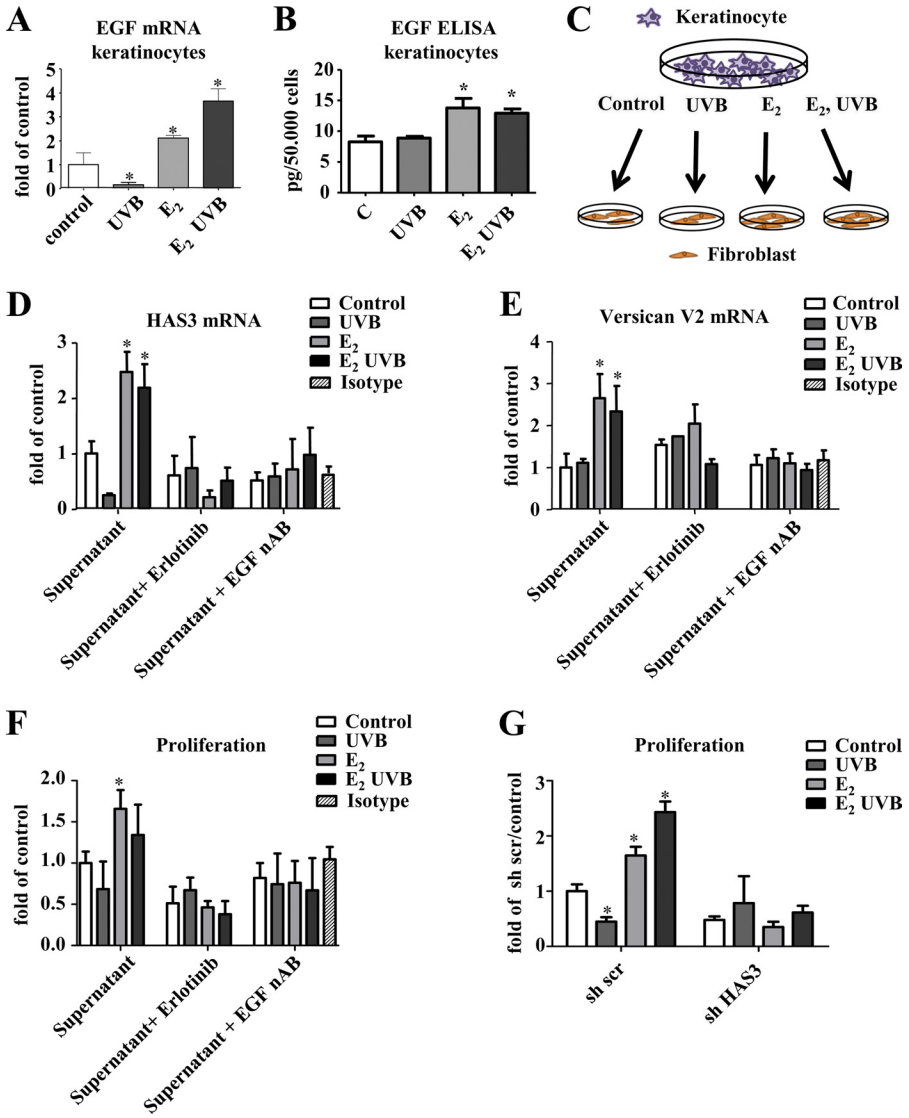

FIGURE 7. **EGF release from keratinocytes in response to E_2 and UVB.** *A,* keratinocytes were treated with 100 nM E_2, 100 mJ/cm^2 UVB, or both. After 24 h, *EGF* mRNA expression was analyzed by real time RT-PCR. *B,* EGF protein was determined by ELISA in cell culture supernatants of keratinocytes treated as described in *A. C,* schematic representation of the experiments shown in *D–G* using keratinocyte-conditioned medium to investigate paracrine EGF effects. *D* and *E,* supernatants as shown in *B* were used to stimulate human skin fibroblasts. After 24 h, *HAS3* mRNA expression and *VERSICAN* V2 mRNA expression were determined by real time RT-PCR in the presence or absence of 3 μM erlotinib, EGF neutralizing antibody (*EGF nAB*, 0.35 μg/ml), or isotype control IgG (0.35 μg/ml). *F,* cell culture supernatants as in *B* were used to stimulate fibroblasts. [^{3}H]Thymidine incorporation was determined as a measure of DNA synthesis and proliferation; *G,* [^{3}H]thymidine incorporation in response to the supernatants as in *B* in fibroblasts pretreated with scrambled or *HAS3*-targeting lentiviral shRNA; $n = 3–6$, mean ± S.E.; *, $p < 0.05$ *versus* control.

might be due to lack of E_2-mediated expression of transforming growth factor β1 (TGFβ1) (39).

Here, EGF displayed an expression pattern in response to E_2 substitution that paralleled the changes of HA and HAS3 both in photoaged skin and in nonirradiated skin. Specifically, *EGF* mRNA and protein showed a trend to reduced expression by OVX and strong induction by E_2. EGF is known to induce the expression of HAS2 and HAS3 in keratinocytes, thereby promoting the pro-proliferative and migratory response to EGF (40, 41). Because skin extracts were used to determine *Egf* mRNA and protein, which reflect epidermis plus dermis, both keratinocytes and fibroblasts might be the source of EGF in response to E_2. However, immunostaining of EGF already suggested a pronounced EGF response in the epidermis. The *in vitro* experiments confirmed that E_2 indeed induced EGF expression in keratinocytes but not in dermal fibroblasts (data not shown). Subsequently, EGF released *in vitro* in response to E_2 and UVB from keratinocytes was shown to stimulate HAS3, versican V2 expression, and proliferation in human skin fibroblasts. The pro-proliferative effect was shown to be dependent on EGF and HAS3 as shown by EGF inhibitors and lentiviral transduction with sh*HAS3*. Therefore, it is proposed that E_2 stimulates keratinocytes to release EGF, which in turn induces HAS3 and versican V2 expression in dermal fibroblasts. The limitation of the *in vitro* experiments is that they reflect an acute response to single UVB irradiation, whereas *in vivo* repetitive chronic dosing of UVB was applied. However, the results are in agreement with the observation in other biologic systems that EGF is involved in various estrogen-induced responses (42, 43) or mimics E_2 responses (44) both *in vitro* and *in vivo*.

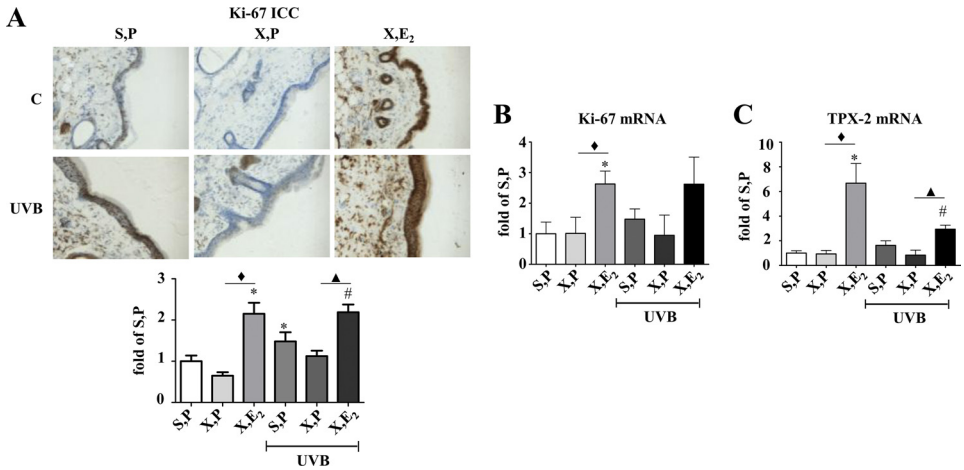

FIGURE 8. **Proliferative responses to E_2 and UVB *in vivo*.** The proliferative response was analyzed in the dermis of skin biopsies derived from 18-week-old hairless skh-1 mice treated as described in the legend of Fig. 1. *A,* immunohistochemistry of Ki-67 and quantitative analysis of the papillary dermis; *B, KI67* mRNA expression; *C, TPX-2* mRNA expression. ×100 magnification; $n = 3–12$, mean ± S.E.; *, $p < 0.05$ *versus* S,P; #, $p < 0.05$ *versus* S,P UVB; ♦, $p < 0.05$ *versus* X,P; ▲, $p < 0.05$ *versus* X,P UVB.

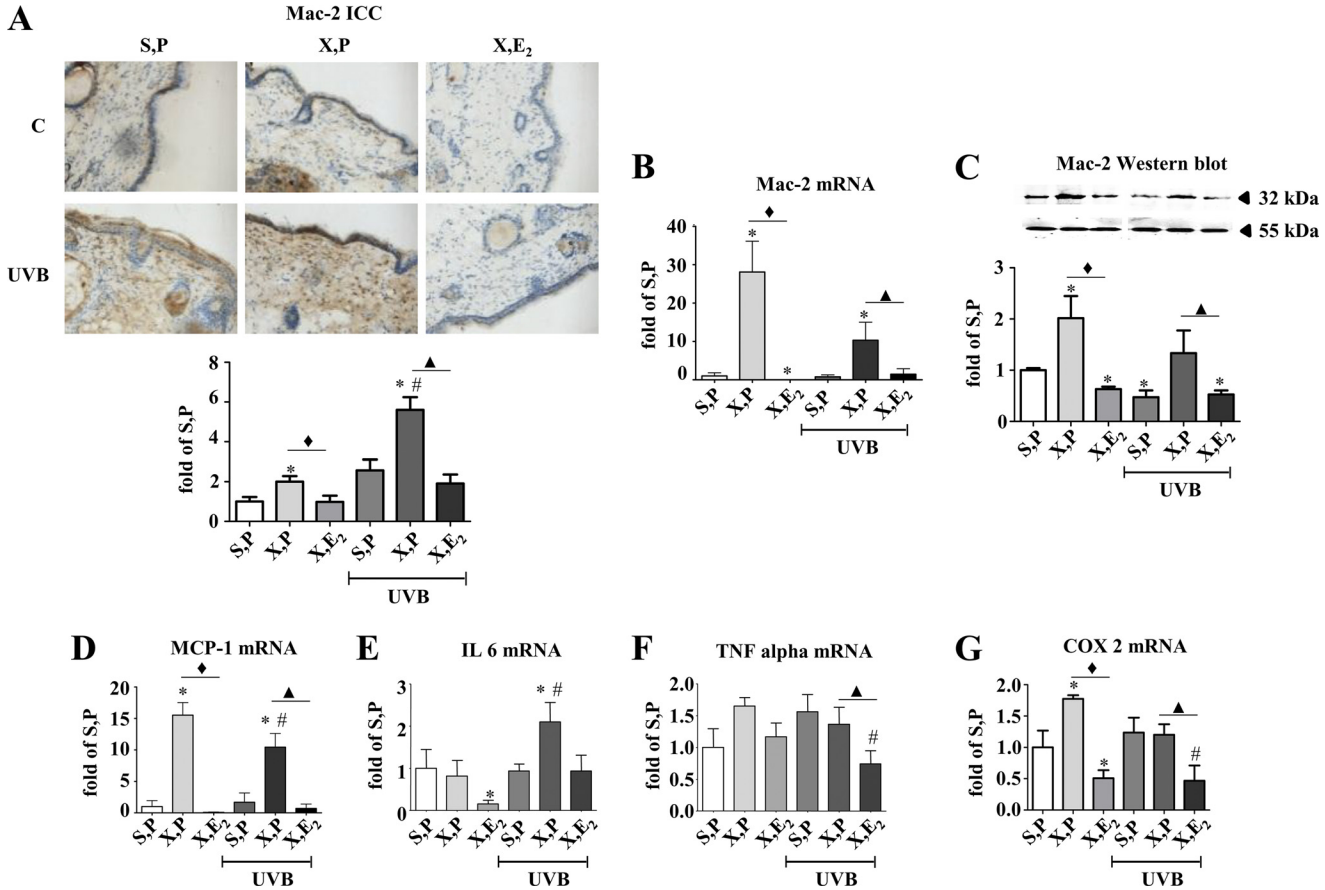

FIGURE 9. **Inflammatory responses to E_2 and UVB *in vivo*.** The inflammatory response was analyzed in the dermis of skin biopsies derived from 18-week-old hairless skh-1 mice treated as described in the legend of Fig. 1. *A,* immunostaining of Mac-2 as marker of inflammatory macrophages; *B, MAC-2* mRNA expression; *C,* Mac-2 immunoblotting and quantification related to tubulin as loading control (55 kDa); *D, MCP-1* mRNA expression; *E, IL6* mRNA expression; *F, TNFα* mRNA expression; *G, COX2* mRNA expression as an inducible gene associated with inflammation and release of inflammatory chemokines and cytokines. ×100x magnification; $n = 3–12$, mean ± S.E.; *, $p < 0.05$ *versus* S,P; #, $p < 0.05$ *versus* S,P UVB; ♦, $p < 0.05$ *versus* X,P; ▲, $p < 0.05$ *versus* X,P UVB.

These findings might also be relevant with respect to the aged phenotype of fibroblasts. Interestingly, age-associated resistance to phenotypic activation of fibroblasts is accompanied by reduced HA synthesis and the failure to up-regulate HA in response to growth factors (45). EGF appears to be involved in this process, because EGF signaling is critically required for TGFβ1-induced HA synthesis (46, 47). Furthermore, fibroblast proliferation is stimulated by EGF, and in aging fibroblasts this proliferative response declines partly due to down-regulation of the EGF receptor (48, 49). Thus, EGF is a growth factor that opposes the aging phenotype of dermal fibroblasts, and this response involves in part HA synthesis and signaling. It is there-

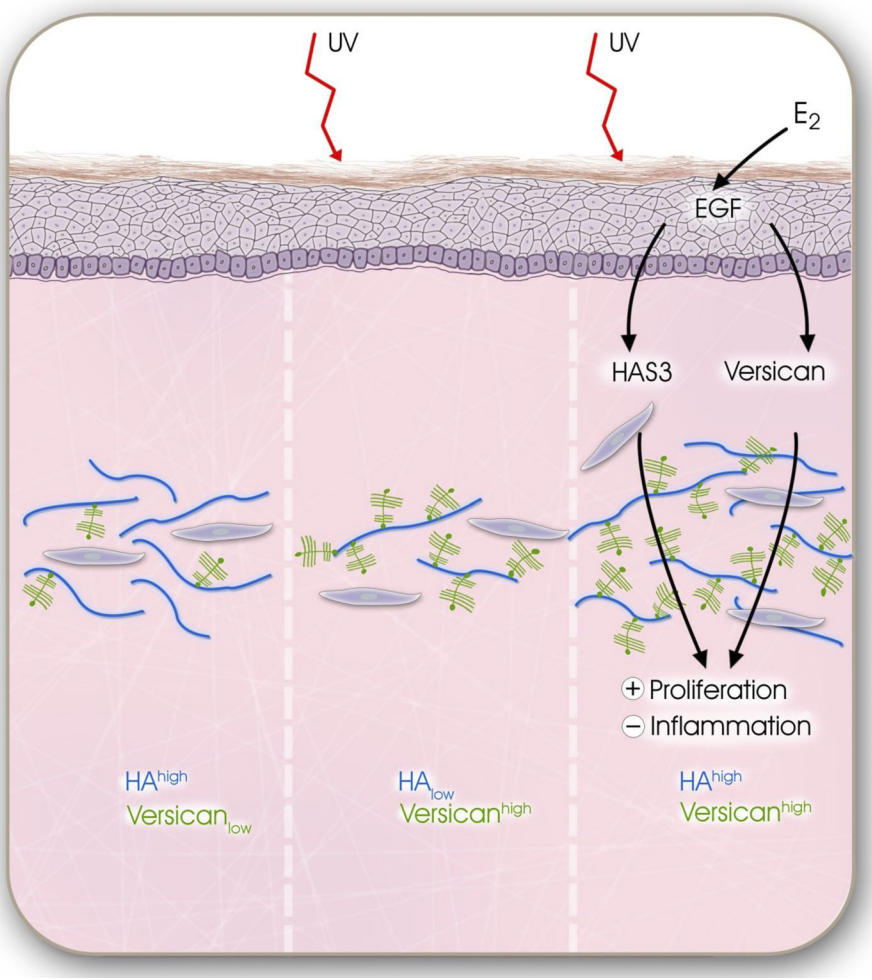

FIGURE 10. **UVB and E_2-mediated remodeling of dermal matrix during extrinsic aging.** Schematic summary of the working hypothesis that was deduced from the presented data is shown. After chronic UVB exposure, the dermal matrix undergoes remodeling from HA-rich and versican-poor matrix with low proliferative and low inflammatory activity (*left panel*) to a HA-low and versican-rich ECM characterized by low proliferative but high inflammatory activity (*middle panel*). E_2 via paracrine release of EGF from the epidermis up-regulates HAS3 and versican that cause transition into HA-rich and versican-rich dermal matrix with higher proliferative activity and reduced inflammation. This E_2-mediated matrix remodeling partially overwrites the UVB-induced degeneration of the dermal matrix possibly setting the stage for skin regeneration due to increased pro-proliferative activity and by inhibition of inflammatory responses.

fore likely that induction of EGF in keratinocytes by E_2 and paracrine stimulation of HAS3 and versican V2 in dermal fibroblasts is involved in the attenuation of the aged fibroblast and skin phenotype by E_2.

In vitro studies have to date provided ample information about the function of individual single matrix components, including collagens, HA, HAS isoenzymes, and versican. However, it is obvious that during physiologic and pathophysiologic responses, changes in matrix composition occur that simultaneously involve multiple matrix molecules. This dramatically affects the cellular microenvironment. Yet cellular responses likely represent the consequences of the combined effects of these complex changes. These include alterations in micromechanic forces and matrix receptor signaling through integrins, the HA receptors CD44 and RHAMM, and activation of alternative receptors by degraded matrix molecules such as toll-like receptors that mediate "danger signals" (50). Therefore, a possibly important finding of this study was that photoaging resulted in a dermal matrix characterized by low HA content and high versican content. At present, it is unknown what the consequence of this shift in the relative abundance of HA and versican may be for the phenotype of cells and the aged phenotype of the skin. It is remarkable, however, that treatment with E_2 increases both HA and versican resulting in a matrix with high HA and high versican content. Versican has four splicing variants that are characterized by loss of glycosaminoglycan-bearing domains and therefore major differences in molecular weight and chondroitin sulfate content (51). The functions of the different splice variants appear to differ, in part opposing each other, in various biologic systems (52). The presented data point toward versican V2 as the target of E_2/EGF-mediated regulation in the skin. Although the dermal function of versican V2 has not been addressed, in the central nervous system it has been suggested to regulate matrix assembly (53). Therefore, versican V2 might be an interesting candidate for regulating matrix assembly and function in skin homeostasis and skin aging.

In this study, the proliferative capacity of fibroblasts in the dermis was positively correlated with increased HA and versican content after E_2 treatment. This is in line with the hypothesis that pericellular matrix consisting of both pericellular HA and versican promotes proliferation (20). *In vitro* knockdown of

HAS3 prevented fibroblast proliferation in response to EGF secreted into conditioned medium from E_2-stimulated keratinocytes. The role of versican splice variant V2 in the E_2 response in the dermis should be addressed in future studies. An additional effect of estrogen was to reduce the content of inflammatory macrophages and the expression of *MCP-1* and *COX2* in nonirradiated and UVB irradiated skin. It is believed that the supramolecular structure of the pericellular matrix and the recruited molecules determine whether the matrix acts homeostatic (5), pro-inflammatory (54, 55), or pro-migratory (20). Therefore, consideration for future studies might be that the ratio of HA and different versican splice variants plays a role in the inflammatory response to UVB in the dermis.

In conclusion, E_2 represents a critical regulator of dermal HA and versican content during photoaging, through release of EGF from keratinocytes, which in turn induces the expression of HAS3 and versican V2 in dermal fibroblasts in a paracrine manner. As a consequence, fibroblast proliferation is increased by E_2, and inflammation is inhibited. Therefore, this study identifies novel molecular targets of E_2 that may contribute to the protective function of this hormone on dermal matrix during intrinsic and extrinsic aging responses.

REFERENCES

1. Fisher, G. J., Datta, S. C., Talwar, H. S., Wang, Z. Q., Varani, J., Kang, S., and Voorhees, J. J. (1996) Molecular basis of sun-induced premature skin aging and retinoid antagonism. *Nature* **379,** 335–339
2. Brennan, M., Bhatti, H., Nerusu, K. C., Bhagavathula, N., Kang, S., Fisher, G. J., Varani, J., and Voorhees, J. J. (2003) Matrix metalloproteinase-1 is the major collagenolytic enzyme responsible for collagen damage in UV-irradiated human skin. *Photochem. Photobiol.* **78,** 43–48
3. Varani, J., Spearman, D., Perone, P., Fligiel, S. E., Datta, S. C., Wang, Z. Q., Shao, Y., Kang, S., Fisher, G. J., and Voorhees, J. J. (2001) Inhibition of type I procollagen synthesis by damaged collagen in photoaged skin and by collagenase-degraded collagen *in vitro*. *Am. J. Pathol.* **158,** 931–942
4. Koshiishi, I., Horikoshi, E., Mitani, H., and Imanari, T. (1999) Quantitative alterations of hyaluronan and dermatan sulfate in the hairless mouse dorsal skin exposed to chronic UV irradiation. *Biochim. Biophys. Acta* **1428,** 327–333
5. Stern, R., and Maibach, H. I. (2008) Hyaluronan in skin. Aspects of aging and its pharmacologic modulation. *Clin. Dermatol.* **26,** 106–122
6. Tammi, R., Agren, U. M., Tuhkanen, A. L., and Tammi, M. (1994) Hyaluronan metabolism in skin. *Prog. Histochem. Cytochem.* **29,** 1–81
7. Knott, A., Reuschlein, K., Lucius, R., Stäb, F., Wenck, H., and Gallinat, S. (2009) Deregulation of versican- and elastin-binding protein in solar elastosis. *Biogerontology* **10,** 181–190
8. Dai, G., Freudenberger, T., Zipper, P., Melchior, A., Grether-Beck, S., Rabausch, B., de Groot, J., Twarock, S., Hanenberg, H., Homey, B., Krutmann, J., Reifenberger, J., and Fischer, J. W. (2007) Chronic ultraviolet B irradiation causes loss of hyaluronic acid from mouse dermis because of down-regulation of hyaluronic acid synthases. *Am. J. Pathol.* **171,** 1451–1461
9. Yoneda, M., Yamagata, M., Suzuki, S., and Kimata, K. (1988) Hyaluronic acid modulates proliferation of mouse dermal fibroblasts in culture. *J. Cell Sci.* **90,** 265–273
10. Itano, N., and Kimata, K. (2002) Mammalian hyaluronan synthases. *IUBMB Life* **54,** 195–199
11. Toole, B. P. (2004) Hyaluronan. From extracellular glue to pericellular cue. *Nat. Rev. Cancer* **4,** 528–539
12. Bourguignon, L. Y., Gilad, E., and Peyrollier, K. (2007) Heregulin-mediated ErbB2-ERK signaling activates hyaluronan synthases leading to CD44-dependent ovarian tumor cell growth and migration. *J. Biol. Chem.* **282,** 19426–19441
13. Karousou, E., Kamiryo, M., Skandalis, S. S., Ruusala, A., Asteriou, T., Passi, A., Yamashita, H., Hellman, U., Heldin, C. H., and Heldin, P. (2010) The activity of hyaluronan synthase 2 is regulated by dimerization and ubiquitination. *J. Biol. Chem.* **285,** 23647–23654
14. Vigetti, D., Genasetti, A., Karousou, E., Viola, M., Clerici, M., Bartolini, B., Moretto, P., De Luca, G., Hascall, V. C., and Passi, A. (2009) Modulation of hyaluronan synthase activity in cellular membrane fractions. *J. Biol. Chem.* **284,** 30684–30694
15. Averbeck, M., Gebhardt, C. A., Voigt, S., Beilharz, S., Anderegg, U., Termeer, C. C., Sleeman, J. P., and Simon, J. C. (2007) Differential regulation of hyaluronan metabolism in the epidermal and dermal compartments of human skin by UVB irradiation. *J. Invest. Dermatol.* **127,** 687–697
16. Ghersetich, I., Lotti, T., Campanile, G., Grappone, C., and Dini, G. (1994) Hyaluronic acid in cutaneous intrinsic aging. *Int. J. Dermatol.* **33,** 119–122
17. Takahashi, Y., Ishikawa, O., Okada, K., Kojima, Y., Igarashi, Y., and Miyachi, Y. (1996) Disaccharide analysis of human skin glycosaminoglycans in sun-exposed and sun-protected skin of aged people. *J. Dermatol. Sci.* **11,** 129–133
18. Schwartz, E. (1988) Connective tissue alterations in the skin of ultraviolet-irradiated hairless mice. *J. Invest. Dermatol.* **91,** 158–161
19. Day, A. J., and Prestwich, G. D. (2002) Hyaluronan-binding proteins. Tying up the giant. *J. Biol. Chem.* **277,** 4585–4588
20. Evanko, S. P., Angello, J. C., and Wight, T. N. (1999) Formation of hyaluronan- and versican-rich pericellular matrix is required for proliferation and migration of vascular smooth muscle cells. *Arterioscler. Thromb. Vasc. Biol.* **19,** 1004–1013
21. Verdier-Sévrain, S., Bonté, F., and Gilchrest, B. (2006) Biology of estrogens in skin. Implications for skin aging. *Exp. Dermatol.* **15,** 83–94
22. Vickers, M. R., MacLennan, A. H., Lawton, B., Ford, D., Martin, J., Meredith, S. K., DeStavola, B. L., Rose, S., Dowell, A., Wilkes, H. C., Darbyshire, J. H., and Meade, T. W. (2007) Main morbidities recorded in the women's international study of long duration estrogen after menopause (WISDOM). A randomized controlled trial of hormone replacement therapy in postmenopausal women. *BMJ* **335,** 239
23. Oppermann, M., Suvorava, T., Freudenberger, T., Dao, V. T., Fischer, J. W. Weber, M., and Kojda, G. (2011) Regulation of vascular guanylyl cyclase by endothelial nitric oxide-dependent post-translational modification. *Basic Res. Cardiol.* **106,** 539–549
24. Twarock, S., Freudenberger, T., Poscher, E., Dai, G., Jannasch, K., Dullin, C., Alves, F., Prenzel, K., Knoefel, W. T., Stoecklein, N. H., Savani, R. C., Homey, B., and Fischer, J. W. (2011) Inhibition of esophageal squamous cell carcinoma progression by *in vivo* targeting of hyaluronan synthesis. *Mol. Cancer* **10,** 30
25. Zhang, B., Xia, H. Q., Cleghorn, G., Gobe, G., West, M., and Wei, M. Q. (2001) A highly efficient and consistent method for harvesting large volumes of high titer lentiviral vectors. *Gene Ther.* **8,** 1745–1751
26. Chang, M. Y., Potter-Perigo, S., Tsoi, C., Chait, A., and Wight, T. N. (2000) Oxidized low density lipoproteins regulate synthesis of monkey aortic smooth muscle cell proteoglycans that have enhanced native low density lipoprotein binding properties. *J. Biol. Chem.* **275,** 4766–4773
27. Papakonstantinou, E., Roth, M., Block, L. H., Mirtsou-Fidani, V., Argiriadis, P., and Karakiulakis, G. (1998) The differential distribution of hyaluronic acid in the layers of human atheromatic aortas is associated with vascular smooth muscle cell proliferation and migration. *Atherosclerosis* **138,** 79–89
28. Sator, P. G., Sator, M. O., Schmidt, J. B., Nahavandi, H., Radakovic, S., Huber, J. C., and Hönigsmann, H. (2007) A prospective, randomized, double-blind, placebo-controlled study on the influence of a hormone replacement therapy on skin aging in postmenopausal women. *Climacteric* **10,** 320–334
29. Sator, P. G., Schmidt, J. B., Sator, M. O., Huber, J. C., and Hönigsmann, H. (2001) The influence of hormone replacement therapy on skin aging. A pilot study. *Maturitas* **39,** 43–55
30. Kanda, N., and Watanabe, S. (2005) Regulatory roles of sex hormones in cutaneous biology and immunology. *J. Dermatol. Sci.* **38,** 1–7
31. Castelo-Branco, C., Duran, M., and González-Merlo, J. (1992) Skin collagen changes related to age and hormone replacement therapy. *Maturitas* **15,** 113–119
32. Grosman, N., Hvidberg, E., and Schou, J. (1971) The effect of oestrogenic

treatment on the acid mucopolysaccharide pattern in skin of mice. *Acta Pharmacol. Toxicol.* **30,** 458–464
33. Uzuka, M., Nakajima, K., Ohta, S., and Mori, Y. (1981) Induction of hyaluronic acid synthetase by estrogen in the mouse skin. *Biochim. Biophys. Acta* **673,** 387–393
34. Bentley, J. P., Brenner, R. M., Linstedt, A. D., West, N. B., Carlisle, K. S., Rokosova, B. C., and MacDonald, N. (1986) Increased hyaluronate and collagen biosynthesis and fibroblast estrogen receptors in macaque sex skin. *J. Invest. Dermatol.* **87,** 668–673
35. Sobel, H., and Cohen, R. A. (1970) Effect of estradion on hyaluronic acid in the skin of aging mice. *Steroids* **16,** 1–3
36. Hall, J. M., Couse, J. F., and Korach, K. S. (2001) The multifaceted mechanisms of estradiol and estrogen receptor signaling. *J. Biol. Chem.* **276,** 36869–36872
37. Verdier-Sevrain, S., Yaar, M., Cantatore, J., Traish, A., and Gilchrest, B. A. (2004) Estradiol induces proliferation of keratinocytes via a receptor-mediated mechanism. *FASEB J.* **18,** 1252–1254
38. Haczynski, J., Tarkowski, R., Jarzabek, K., Slomczynska, M., Wolczynski, S., Magoffin, D. A., Jakowicki, J. A., and Jakimiuk, A. J. (2002) Human cultured skin fibroblasts express estrogen receptor α and β. *Int. J. Mol. Med.* **10,** 149–153
39. Ashcroft, G. S., Dodsworth, J., van Boxtel, E., Tarnuzzer, R. W., Horan, M. A., Schultz, G. S., and Ferguson, M. W. (1997) Estrogen accelerates cutaneous wound healing associated with an increase in TGF-β1 levels. *Nat. Med.* **3,** 1209–1215
40. Pienimaki, J. P., Rilla, K., Fulop, C., Sironen, R. K., Karvinen, S., Pasonen, S., Lammi, M. J., Tammi, R., Hascall, V. C., and Tammi, M. I. (2001) Epidermal growth factor activates hyaluronan synthase 2 in epidermal keratinocytes and increases pericellular and intracellular hyaluronan. *J. Biol. Chem.* **276,** 20428–20435
41. Pasonen-Seppänen, S., Karvinen, S., Törrönen, K., Hyttinen, J. M., Jokela, T., Lammi, M. J., Tammi, M. I., and Tammi, R. (2003) EGF up-regulates, whereas TGF-β down-regulates, the hyaluronan synthases Has2 and Has3 in organotypic keratinocyte cultures. Correlations with epidermal proliferation and differentiation. *J. Invest. Dermatol.* **120,** 1038–1044
42. Ignar-Trowbridge, D. M., Nelson, K. G., Bidwell, M. C., Curtis, S. W., Washburn, T. F., McLachlan, J. A., and Korach, K. S. (1992) Coupling of dual signaling pathways. Epidermal growth factor action involves the estrogen receptor. *Proc. Natl. Acad. Sci. U.S.A.* **89,** 4658–4662
43. Nelson, K. G., Takahashi, T., Bossert, N. L., Walmer, D. K., and McLachlan, J. A. (1991) Epidermal growth factor replaces estrogen in the stimulation of female genital tract growth and differentiation. *Proc. Natl. Acad. Sci. U.S.A.* **88,** 21–25
44. Gehm, B. D., McAndrews, J. M., Jordan, V. C., and Jameson, J. L. (2000) EGF activates highly selective estrogen-responsive reporter plasmids by an ER-independent pathway. *Mol. Cell. Endocrinol.* **159,** 53–62
45. Webber, J., Meran, S., Steadman, R., and Phillips, A. (2009) Hyaluronan orchestrates transforming growth factor-β1-dependent maintenance of myofibroblast phenotype. *J. Biol. Chem.* **284,** 9083–9092
46. Simpson, R. M., Wells, A., Thomas, D., Stephens, P., Steadman, R., and Phillips, A. (2010) Aging fibroblasts resist phenotypic maturation because of impaired hyaluronan-dependent CD44/epidermal growth factor receptor signaling. *Am. J. Pathol.* **176,** 1215–1228
47. Simpson, R. M., Meran, S., Thomas, D., Stephens, P., Bowen, T., Steadman, R., and Phillips, A. (2009) Age-related changes in pericellular hyaluronan organization leads to impaired dermal fibroblast to myofibroblast differentiation. *Am. J. Pathol.* **175,** 1915–1928
48. Shiraha, H., Gupta, K., Drabik, K., and Wells, A. (2000) Aging fibroblasts present reduced epidermal growth factor (EGF) responsiveness due to preferential loss of EGF receptors. *J. Biol. Chem.* **275,** 19343–19351
49. Reenstra, W. R., Yaar, M., and Gilchrest, B. A. (1993) Effect of donor age on epidermal growth factor processing in man. *Exp. Cell Res.* **209,** 118–122
50. Stern, R. (2004) Hyaluronan catabolism. A new metabolic pathway. *Eur. J. Cell Biol.* **83,** 317–325
51. Wight, T. N. (2002) Versican. A versatile extracellular matrix proteoglycan in cell biology. *Curr. Opin. Cell Biol.* **14,** 617–623
52. Sheng, W., Wang, G., Wang, Y., Liang, J., Wen, J., Zheng, P. S., Wu, Y., Lee, V., Slingerland, J., Dumont, D., and Yang, B. B. (2005) The roles of versican V1 and V2 isoforms in cell proliferation and apoptosis. *Mol. Biol. Cell* **16,** 1330–1340
53. Dours-Zimmermann, M. T., Maurer, K., Rauch, U., Stoffel, W., Fässler, R., and Zimmermann, D. R. (2009) Versican V2 assembles the extracellular matrix surrounding the nodes of Ranvier in the CNS. *J. Neurosci.* **29,** 7731–7742
54. Evanko, S. P., Potter-Perigo, S., Bollyky, P. L., Nepom, G. T., and Wight, T. N. (2012) Hyaluronan and versican in the control of human T-lymphocyte adhesion and migration. *Matrix Biol.* **31,** 90–100
55. de La Motte, C. A., Hascall, V. C., Calabro, A., Yen-Lieberman, B., and Strong, S. A. (1999) Mononuclear leukocytes preferentially bind via CD44 to hyaluronan on human intestinal mucosal smooth muscle cells after virus infection or treatment with poly(IC). *J. Biol. Chem.* **274,** 30747–30755